Production and characterization of silica nanoparticles from rice husk

Daniel F. Hincapié Rojas[1*, 3], Posidia Pineda Gómez[1, 2], Andrés Rosales Rivera[1]

[1]*Laboratorio de Magnetismo y Materiales Avanzados, Facultad de Ciencias Exactas y Naturales, Universidad Nacional de Colombia, Caldas, Manizales, 170001, Colombia*
[2]*Departamento de Física, Universidad de Caldas, Manizales, 170001, Colombia*
[3]*Departamento de Física y Matemáticas, Universidad Autónoma de Manizales, Manizales, 170001, Colombia*

*Corresponding author: Tel: (+57) 3153483374; E-mail: daniel.hincapier@autonoma.edu.co

DOI: 10.5185/amlett.2019.2142
www.vbripress.com/aml

Abstract

The rice process generates a large amount of husk, which can become an environmental contaminant if it does not receive an adequate management. Because rice husk is a natural source of silica, in this work silica nanoparticles were obtained as an alternative use for this residue. The synthesis was carried out with the incineration, acid leaching process, and particle size reduction through high-energy mechanical ball milling. For its characterization, thermal, chemical, morphological, structural and superficial area analyses were performed with thermogravimetric analysis, X-ray fluorescence method, scanning electron microscopy, transmission electron microscopy, X-ray diffraction, and Nitrogen adsorption/desorption isotherm techniques. The results indicated that between 150-450°C the organic material of the rice husk was released, and above 550°C was obtained ash rich in silica. The silica purity was effectively increased to 98.48%, through acid leaching with acid nitric. The reduction of particle size by mechanical milling at 600 rpm for 3 h was achieved up to nanometer size. Most of the nanoparticles were spherical with a diameter between 14 and 28 nm. Silicon oxide was the principal structural phase of the nanoparticles corroborated by the broad peak corresponding to the (101) plane shown by XRD pattern. A substantial increase of two magnitude orders of the specific surface area of nanoparticles was reached in comparison with particles without milling. The nanosilica particles obtained from rice husk can be used for the production of high-performance silicon or they can be also used as supplementary cementitious materials.

Keywords: Rice husk, Nanosilica, NPs, mechanical ball milling, chemical treatment.

Introduction

Rice is one of the major crops grown throughout the world since it is one of the principal food and a provider of nourishment for people [**1**]. According to the United Nations Food and Agriculture Organization (FAO), the global production of rice in the year 2016 was 748.0 million tones [**2**]. Rice husk (RH) constitutes as the major residue as result of production and refinement in this agricultural industry [**3-6**]. About one-fifth of the gross weight of the grain corresponds to husk, it means that around 150 million tons of RH are produced each year [**6**]. Because of its hard surface, high silicon content, low level of proteins, and lignin content, rice husk cannot be easily decomposed by bacteria [**7**]; additionally, it is not soluble in water. In several countries, most of RH is vainly burned thereby resulting in pollution problems [**8**], or it is dumped into water sources, which causes a release of methane during its decomposition and thus contaminates the environment and affects people's health [**9-11**]. Undoubtedly, water scarcity and pollution are the most urgent environmental issues for the 21st century. The agricultural waste biomass is one of the most challenging topics for reducing pollution to the environment [**1**]. Finding a most efficient use of the byproduct of the rice industry is pertinent. Rice husk is a biphasic material composed of organic (75-90%) and inorganic (10-25%) components [**10**]. The cellulose, hemicellulose, and lignin are the majority organic constituents. The proportion of organic/inorganic depends on the rice variety, climatic conditions, and geographic location of cultivation [**12**]. When rice husk is burned, the remaining ash contains about 95% is of silica and other minor amounts of metallic elements (inorganic impurities) such as MgO, CaO, Fe_2O_3, Al_2O_3, K_2O, and P_2O_5. [**6, 10-14**]. These impurities can be turned into soluble ions through acid treatment to be removed by filtration in order to obtain the ash-rich in silica [**13**]. In reason of the above, rice husk is considered to be the most economically important natural source of silica [**3**], which is highly porous, pure, and lightweight [**15**]. Silica is frequently used as a Portland cement additive to obtain pozzolanic material,

among other uses [**16-22**]. The use of agricultural biomass in the production of pozzolanic material is considered technically feasible and has been the focus of recent studies. Because of the accumulation of agricultural waste, has increased environmental concern. Using biomass as raw material instead of conventional ones offers a substantial environmental contribution, helping to reduce the problems of pollution and conservation of natural resources for future generations [**23**].

Many materials have advantages when they are reduced to nanometer size [**23**]. In the past decade, novel properties of nanoparticles (NPs) with 1–100 nm scale have attracted enormous interest due to their potential new uses [**24**]. The nanoparticles can improve properties from conventional grain-size materials of the same chemical composition [**25**]. With the development of new materials reaching unprecedented levels, it allows for the ability to find novel functions for such materials. Some authors such as Hui *et al.* [**25**] have reported the use of nanoparticles in cement-based building materials, to explore their mechanical and smart potentials (temperature and strain sensing). Amorphous silica powder is a basic raw material that is used in many applications [**7, 13, 26-28**]. Silica extracted from rice husk can be employed as an excellent source in the preparation of silica NPs [**27**]. Due to its nanometer size and high superficial area, silica NPs can be attractive for a wide range of applications, such as adsorption materials, filler in composite materials, medical additives, reinforcement of polymers to increase the hardness, modulus, weatherability, flammability, and so on [**26**].

There are several reports for the extraction of pure silica from rice husk ash such as sol-gel, vapor-phase reaction, thermal decomposition technique, thermal pyrolysis, chemical precipitation and biotransformation method [**6, 29**], chemical treatment using acid and base solutions [**30**], among others [**31, 32**]. Nevertheless, these processes are expensive, complex or require a large amount of energy. For this reason, it is interesting to develop versatile and alternative methods for obtaining nanosilica from such biomass. The ball milling method, in comparison with other methods, has many advantages such as effectiveness, high purity of products, moderate reaction temperature, controllability, ease, and reproducibility [**33**]. Nowadays, more work is required for the implementation of efficient methods; therefore, finding an inexpensive way to produce silica NPs from recycling sources great significance and addition to the efforts to protect the environment, since an alternative use is proposed for rice husks, which is a waste that requires adequate management to avoid contamination [**34**].

The purpose of this work was to obtain silica from rice husk waste and then convert it into silica nanoparticles through mechanical ball milling. The purity of the silica, the thermal behavior and the structural properties, the morphological changes and the reduction of particle size, were studied in relation to the mechanical milling time.

Materials and methods

Materials

Rice husk was collected from the central zone of Colombia (Tolima town in June of 2016). This raw material was washed four times with water to remove any soluble adhered particles, dust or any other contaminants such as heavy impurities. Then it was dried in the oven at 100°C for 3 h.

Obtaining silica nanoparticles

The dried rice husk was burnt in a conventional furnace by applying a rate of 5°C/min to reach 550°C; this temperature was maintained for 1 hour to remove organic material. Then the sample was heated until 700°C and was maintained isothermally for 1 h to reduce the carbonaceous materials. This ash was leached to remove impurities through the chemical reaction between the acid and the inorganic impurities, during filtration [**3**]. Nitric acid HNO_3 was purchased from Colombia Bioquigen Ltd., which was analytically pure, the acid was used in a solution at 1.0M. A mix with 15.0 g of ash and 250 ml of the solution was prepared and magnetic stirring at 90°C for 1h was applied. The obtained paste was washed four times with distilled water, filtered and dried in a conventional oven at 100°C for 3h. These reacted metals were leached with the acidic solution. After the leaching process, a white powder rich in silica was obtained.

For obtaining silica nanoparticles, a Gear-Drive 2-Liter Planetary Ball Mill equipped with a high alumina container was employed. Spheres of high-density alumina with an 8 mm diameter as a grinding medium were required where a ratio of 20:1 (spheres: powder) was used at a frequency of 600 rpm in a high-energy planetary ball mill. Three samples were prepared by varying the milling time: sample 1 named S-0 that corresponds to silica without milling process; sample 2 named S-1 that corresponds to silica with 1 h of milling; and sample 3, named S-3 which corresponds to silica milled for 3 h.

Methods of characterization

Thermogravimetric analysis (TGA)

The analysis of the thermal properties of the rice husk was performed using the TGA Q500 equipment (TA Instruments, USA). The samples of 5.8 ± 1.0 mg were placed in the platinum crucible of a thermobalance where a heating rate of 10°C/min was applied from room temperature to 700°C for all the samples. The runs were carried out in an air atmosphere, with the gas flow maintained at 60 mL/min. A TGA Q500 TA Instruments thermobalance was used for the TG analysis of the aforementioned samples. The TG data was processed using the Universal Analysis 2000 TA-

software. The maximum rate of the reaction was determined by the peak temperature in the DTG curve.

X-Ray fluorescence analysis (XRF)

X-Ray Fluorescence analysis was used in order to determine the chemical composition of the ash. Previously, the dried sample was powdered to 270 mesh size (ASTM) and was dried at 105°C for 12 hours. Then, the powder samples were mixed with spectrometric wax (Merck & Co.) with a ratio of 10:1 (Sample:Wax). The slurry was homogenized by means of stirring and compacted to generate pellets with a diameter of 37mm, for the resulting analysis. The semi-quantitative analysis was performed with the software SemiQ making 11 scans to detect components. This kind of analysis cannot quantify light elements such as carbon, nitrogen, oxygen, fluorine and transuranic ones. The x-ray fluorescence spectrometer, Philips MagixPro PW-2440 equipped with the rhodium tube with a maximum power of 4 kW was employed. The equipment had a sensitivity of 200 ppm (0.02%) in the detection of heavy metal elements. Two samples were analyzed, the first was prepared without chemical treatment and the second was leached with nitric acid.

Morphological analysis by Scanning Electron Microscopy (SEM)

A high vacuum scanning electronic microscope JEOL JSM 5910 LV was used with 15.0 kV electron acceleration voltage, in order to know the morphology of the silica nanoparticles. Prior to the analysis, the silica samples were fixed to a copper specimen held on to carbon adhesive tape. A gold layer was deposited by sputtering on a silica surface to make them conductive.

Morphological analysis by Transmission Electron Microscopy (TEM)

In order to know the size of silica NPs, TEM micrographs were recorded using a FEI Tecnai T12 system operating at 120kV. The silica nanoparticles were dropped on Lacey Film-Coated Grids supported by a carbon film. A computer program (Image J) was employed to determine the particle size histogram.

Structural Analysis by X-Ray Diffraction (XRD)

The structure and phases of nanosilica were identified using a RIGAKU diffractometer, MINIFLEX II operated at room temperature, equipped with a Cu Kα radiation source (λ = 1.540562 Å), and a 30 kV and 15 mA X-ray source. Measurements were run from 5° and 70° on a 2θ scale with a step size of 0.02 degrees/s.

Specific surface area by BET

The specific surface area (S_{BET}) of the silica NPs was determined by nitrogen adsorption-desorption isotherms measured with a Micromeritics ASAP 2020 apparatus. Before the analysis, the samples were heated at 100°C for 24 h. The specific surface area of the particles was estimated by the BET method (Brunauer, Emmett and Teller method) using N_2 adsorption isotherm data. The analysis was performed by taking 5 points at relative pressures between 0.05-0.30 at 300°C with a pressure of 3μmHg.

Results and discussion

Thermal properties by Thermogravimetric analysis

Thermogravimetric analysis of rice husk

Rice husk is composed of inorganic and organic materials. Each one of these compounds behave differently at high temperatures. This behavior can be seen using thermogravimetric analysis TGA, which is considered an important tool for the identification and characterization of materials. The weight changes occurred during the combustion of the rice, they were shown by the TGA curve shown in **Fig. 1**. The insert in this figure shows the corresponding derivative profile DTGA that gives the rate of change of mass loss as temperature rises. There are three stages in the DTGA according to the peaks associated with the mass changes which were identified as stage 1, from room temperature to 140°C; stage 2, between 150 and 350°C; and stage 3, between 350 and 500°C. In the first step, the TGA shows an initial weight loss of 5.87%, identified as the moisture due to the elimination of physically absorbed water by the porosity of rice husk; external water bounded by surface tension and light volatiles [**35**]. The second stage corresponding to the highest peak in DTGA was related to the active pyrolysis. The weight loss in this stage (48.05%) can be attributed to the release of volatiles as carbon, oxygen, and hydrogen which are removed from the organic component during the decomposition of cellulose and hemicellulose; condensable vapors (acetic acid, methanol, and wood tare), and incondensable gas (CO, CO_2, CH_4, H_2 and H_2O) are released at this point [**35**]. During stage 3, weight loss (20.14%) can be attributed to the lignin decomposition and the elimination of residual volatiles left from the previous stages (below 400°C); this process corresponds to passive pyrolysis [**27, 28**]. Finally, after 550°C, the mass remained stable and the residual ash corresponded to 25.57% of the total weight which was measured. This residue consists principally of silica SiO_2 and other metallic compounds, as was verified in XRF analysis later.

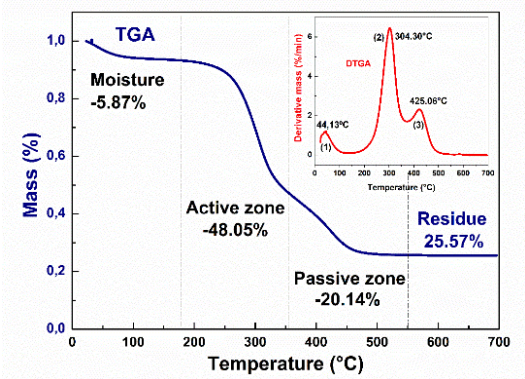

Fig. 1. TGA and DTGA curves obtained by heating the rice husk at 10°C/min in air atmosphere.

In relation to these results and according to Mansaray *et al.*, [**35**], the three main constituents of the lignocellulosic materials (hemicellulose, cellulose and lignin) are chemically active and decompose thermochemically in the temperature range between 150°C and 500°C. The decomposition starts with hemicellulose between 150 and 350°C, followed by cellulose between 275-350°C and finally lignin. In addition, the hemicellulose and cellulose decompose to produce an abundance of organic compounds, such as wood tar, ketone and methanol, which would vaporize by adsorbing high heat. On the other hand, while the lignin undergoes gradual decomposition between 250°C and 500°C, it is mainly responsible for the char portion of the product [**36**].

Thermogravimetric analysis of silica particles

The silica nanoparticles obtained from mechanical milling were also studied by thermogravimetry analysis in order to evaluate the thermal stability of the material when it is subjected to an increase in temperature. This results were compared with the control sample (silica particles without mechanical ball milling process). The figure 2(a-b) shows the TGA curve and also its DTGA derivative for silica particles without milling process and milled at 600 rpm for 3h, respectively. From the thermogram in **Fig. 2(a)** it can be seen that the silica sample without milling had no mass loss during heating, this indicates the stability of this material. However, in **Fig. 2(b)**, it was observed that the silica milled at 600 rpm for 3h, showed an initial mass loss of 5.42% between 25 and 160°C, which can be attributed to humidity caused by porosity of the sample. It should be noted that such porosity could be induced by the increase in surface area associated as a results of the decrease in particle size at nanometric scale.

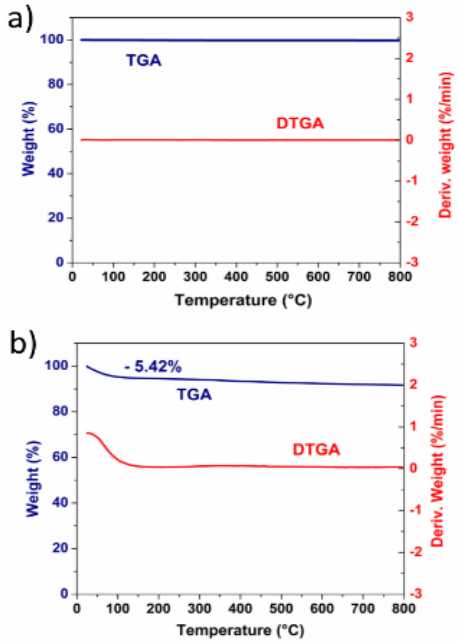

Fig. 2. TGA and DTGA curves at 10ºC/min in air atmosphere: a) silica without milling and b) silica milled at 600 rpm–3h.

X-Ray fluorescence analysis (XRF) of rice husk ash

Inorganic elements have a substantial effect on the quality of silica. Therefore, it was necessary to treat the ash with an acidic solution, in order to diminish some impurities and to obtain a highly purified silica powder. X-ray Fluorescence (XRF) was used to obtain the chemical composition of ash without chemical treatment, as well as sample leached with acid nitric. **Table 1** shows the effect of acid treatment in the elimination of impurities on the ash samples, the test were done by triplicate. The main impurities present in the ash sample were MgO, CaO, Fe_2O_3, Al_2O_3, K_2O, and P_2O_5. The acid leaching process substantially decreased the level of these impurities, the acid converted the metallic elements into soluble ions and they were subsequently eliminated by filtration. Before the acid leaching, the silica content in the ash was 93.38%, after the treatment the content increased to 98.47%, thus indicating that the impurities represented, mainly metallic oxides, were eliminated [**21**].

Table 1. Chemical composition of rice husk ash with and without chemical treatment.

Element and/or compound	Without chemical treatment (%)	Leached with nitric acid (%)
SiO_2	93.40 ± 0.02	98.47 ± 0.04
CaO	0.70 ± 0.02	0.25 ± 0.01
K_2O	0.68 ± 0.01	0.63 ± 0.01
P_2O_5	0.59 ± 0.01	0.04 ± 0.00
MgO	0.26 ± 0.01	0.21 ± 0.01
Al_2O_3	0.21 ± 0.03	0.10 ± 0.02
MnO	0.14 ± 0.01	0.10 ± 0.01
Fe_2O_3	0.09 ± 0.01	0.08 ± 0.01
SO_3	0.07 ± 0.01	0.04 ± 0.01
Na_2O_3	0.02 ± 0.00	0.03 ± 0.01
$Others$	3.84 ± 0.01	0.05 ± 0.01

Morphological analysis by scanning electron microscopy

After the chemical treatment, the samples were submitted to high-energy mechanical milling; later, the morphological analysis was conducted. Scanning electron microscopy (SEM) and transmission electron microscopy (TEM) are two major methods that can be used to determine the morphology and detailed structures of many nanomaterials. **Fig. 3** shows the micrographs SEM of the three samples taken as 20000X. The sample without the milling process (S-0) showed larger grains, even with particle agglomerates that reach approximately 10 microns. On the other hand, the samples S-1 and S-3 showed a drastic decrease in the particle size, this fact is due to the effect of high-energy ball milling. The sample S-1 shows cumulus ranging from the submicron size up to 4 microns. Nevertheless, the sample S-3 presents the smallest particle size, with agglomerates and particles in nano-metric dimensions. If the material is subjected for longer to the collisions, intensive fracturing and

welding generated in the milling process a reduction in the mean particle size could achieved [**34**]. Nanometric sizes were verified in the powder after 3 h milling time so that the mechanical ball milling showed to be effective for to obtain silica nanoparticles.

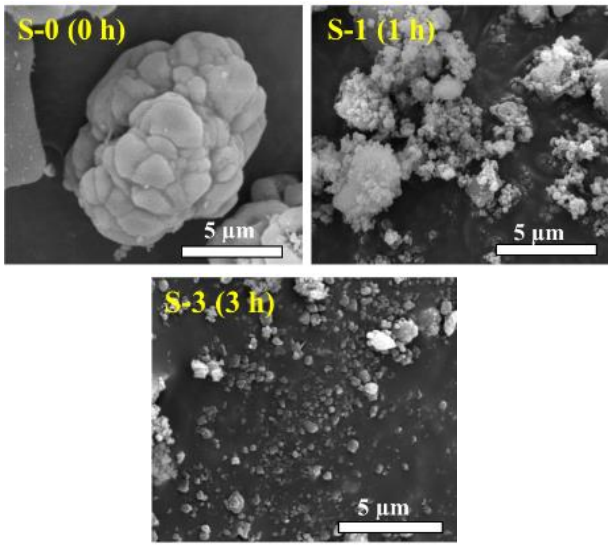

Fig. 3. SEM images of silica particles and NPs at 20000X.

A detailed view at 40000X of the samples S-1 and S-3 is shown in **Fig. 4**. The sample S-3 presents a finer grain size, the average particle size is less than 500 nm, it means that silica NPs can be achieved as will be shown below with the TEM. These results corroborate that there was a drastic decrease in the average particle sizes to nano-dimensions by milling at higher speeds (600 rpm) compared with the sample without milling. The effect of high-energy ball milling was corroborated.

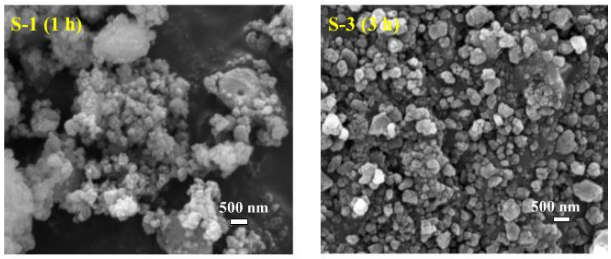

Fig. 4. SEM micrographs taken at 40000X of the formed silica NPs.

Morphological analysis by transmission electron microscopy

The size and shape, uniformity, and homogeneity of silica NPs were further analyzed by using TEM. **Fig. 5(a)** exhibits the nanoparticles corresponding to sample S-3. The software ImageJ gave the histogram for size distribution as can be seen in **Fig. 5(b)**. An approximation Log-normal curve is aggregated in the histogram. Silica NPs with approximately spherical shapes are within nano-dimensions with a diameter between 14 and 28 nm. The majority population was observed with a size of 21 nm. The presence of agglomerates can also be seen, this inevitable phenomenon is associated with the interaction between particles of small size due to electrostatic attraction or Van der Walls forces [**37**]. The small size of the silica NPs obtained indicates that they can be usefully exploited in suitable applications.

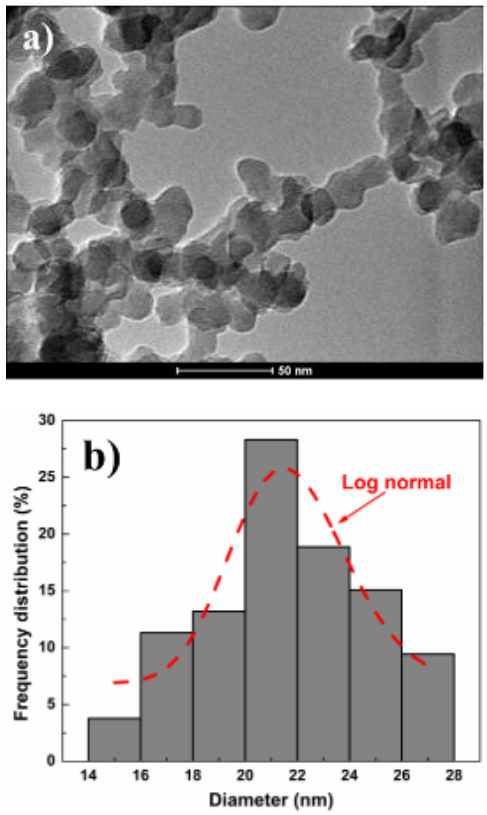

Fig. 5. (a) TEM micrographs of the formed silica NPs, (b) Particle size distribution of NPs.

Structural analysis by X-Ray diffraction

X-Ray diffraction is a very important technique for identification of the crystalline structure of the materials. The X-ray diffraction pattern of the sample without milling (S-0) and the sample prepared after 1 hour (S-1), and 3 hours (S-3) are shown in **Fig. 6**. The initial patterns (S-0) were compared with powder diffraction file PDF#00-011-0695 of silicon oxide SiO_2. In the diffractograms, the arrows correspond to the main diffracted peaks. The most prominent peak was identified in 2θ=22.01° corresponding to (101) plane. The effect of milling was corroborated. For 1 hour of milling, some peaks disappeared ((111), (102), (113), (212), (301)) and others were widened and with less intensity ((101), (200)), it indicated that crystallinity of the silica was reduced, as a consequence of the mechanical milling process. Increasing the milling time to 3 hours, a very broad peak corresponding to the (101) plane was observed, which is characteristic of a material in nanometric scale, this broadening could be associated with the scaterring caused by nanoparticles. Because the amorphous broad peak is located at the main peak of (101) plane of silicon oxide crystalline, the phase can be considered as an amorphous SiO_2 [**33,**

38, 39]. These results suggest that a decrease in the order of the crystalline structure is related to the micro strain generated in the high-energy ball milling process.

The broadening of XRD peaks is associated with both crystallite size refinement and increase of micro strains presents in the material. In order to determine the influence of the milling time on the structure, the FWHM (Full width at half maximum) of the high intensity peak and the crystallite size for samples S-0 and S-1 were calculated. The FWHM were obtained using a Gaussian model, the values obtained were 0.17° and 0.45° respectively. The increased of these values can be correlated with the structural changes in the samples, because the mechanical ball milling introduces stress, generates structural distortions, increase the density defect points that manifest itself with the widening of the diffraction peaks. On the other hand, it is well known, the mechanical alloying process involves a decrease in crystallite size. For this reason, the crystallite size were calculated through Debye-Scherrer equation [**40**], the values obtained for S-0 and S-1 were 37.15 and 17.34 nm respectively. The effect of mechanical ball milling was corroborated. However, the results of the structural analysis for the S-3 sample show the presence of a single very broad (see **Fig. 6**); therefore the calculated value of the FWHM and the crystallite size has not physical meaning.

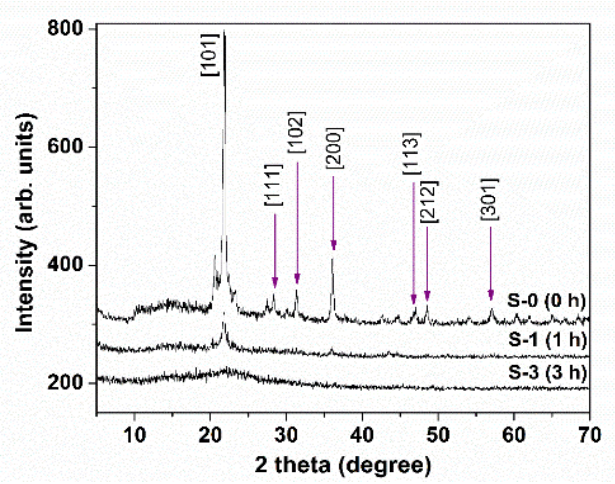

Fig. 6. XRD patterns: silica without milling, silica milled for 1 or 3 h.

Specific surface area by BET

The nanoparticles NPs are different from the bulk phase of the same material because they contain more available surface [**41**]. The NPs' surfaces tend to have softer vibration modes than the bulk and so have thermal properties that operate at lower temperatures. The role of the surface can be used to explain the structure measure, the lattice constant and surface stresses [**41**]. The specific surface area was measured to compare the milling effect. As raw material silica S-0 (without milling) presented a specific surface area of 1.15 ± 0.11 m²/g. After the mechanical ball milling for 3 h at 600 rpm (sample S-3), the material was reduced to nanometric size (14 to 28 nm) and the specific surface area increased to 148.19 ± 2.88 m^2/g. This means that silica NPs had a surface area 100 times greater in comparison to particles from the raw material. This surface area is consistent with results of microstructural characterization. These results show that silica NPs here synthesized can be attractive for various engineering applications especially in the reinforcement of materials, among other uses.

Conclusion

In this work an alternative and efficient method was developed to obtain silica nanoparticles from the incineration of the rice husk waste and high-energy mechanical ball milling of their ash. The treatment with nitric acid proved to be effective for the elimination of impurities in the ash generating an increase of 5% in the purity; the residual ash had a composition of 98.22% silicon oxide. The high-energy mechanical milling process at 600 rpm during 3 h proved to be effective in reducing the average particle size. Nanometric particle sizes were reached with diameters between 14 and 28 nm which were verified by TEM. This reduction led to an increase of two orders of magnitude in the surface area of the nanoparticles in comparison with particles without milling, which was corroborated by the BET method. X-ray diffraction showed that silicon oxide was the principal structural phase of the nanoparticles, where the predominant peak occurred at 22.09 degrees (2 theta scale); however, a large widening in this peak was observed, it is characteristic by nano-sized materials. In this case, the scattering associated to the nanoparticles was superposed with the diffraction signal. These nanoparticles with a large surface area can be used for example, as additives for the cement due to their high pozzolanic reactivity.

Acknowledgement

We thank Professor E. R. Parra, Professor P.J. Arango and Eng. Lina by X-ray diffraction, G. A. Bolaños for SEM studies and D. V. Marin Castaño and P. Marin Castaño for SBET and TEM studies. We also thank Professor J. Roa from Universidad Nacional de Colombia, sede Bogotá who supplied the milling equipment.

Disclosure statement

No potential conflict of interest was reported by the author.

References

1. Foo, K. Y.; Hameed, B. H., *Adv. Colloid Interface Sci.*, **2009,** *152*, 39.
2. Food and Agricultural Organization of the United Nations, "Diciembre de 2016," **2016**.
3. Liou, T. H.; Chang, F. W.; Lo, J. J., *Ind. Eng. Chem. Res.*, **1997,** *36*, 568.
4. Zhang, H.; Ding, X.; Chen, X.; Ma, Y.; Wang, Z.; Zhao, X., *J. Hazard. Mater.*, **2015,** *291*, 65.
5. Salas, A.; Ospina, M. A.; Delvasto, S.; De Gutierrez, R. M., "Study on the pozzolanic properties of silica obtained from rice husk by chemical and thermal process," **2007**, *4318*, 4311.
6. Tolba, G. M. K.; et al., *J. Ind. Eng. Chem.*, **2015**, *29*, 134.
7. Noushad, M.; Rahman, I. A.; Sheeraz, N.; Zulki, C.; Husein, A.; Mohamad, D., *Ceram. Int.*, **2014**, *40*, 4163.
8. Della, V. P.; Kühn, I.; Hotza, D., "Rice husk ash as an alternate source for active silica production," *Mater. Lett.*, **2002**, *57*, 818.

9. Prasetyoko, D.; Ramli, Z.; Endud, S.; Hamdan, H.; Sulikowski, B., "Conversion of rice husk ash to zeolite beta," Waste Manag., **2006**, *26*, 1173.
10. Carmona, V. B.; Oliveira, R. M.; Silva, W. T. L.; Mattoso, L. H. C.; Marconcini, J. M., "Nanosilica from rice husk: Extraction and characterization," Ind. Crops Prod., **2013**, *43*, 291.
11. Shen, Y.; Zhao, P.; Shao, Q., *Microporous Mesoporous Mater.*, **2014**, 188, 46.
12. C. of P. F. with Guo, C.; Husk, T. R.; Zhou, L.; Lv, J., *Polym. Polym. Compos.*, **2013**, *21*, 449.
13. Zhang H.; et al., *Bioresour. Technol.*, **2010**.
14. Deiana, C.; Granados, D.; Venturini, R.; Amaya, A.; Sergio, M.; Tancredi, N., *Ind. Eng. Chem. Res.*, **2008**, *47*, 4754.
15. C. Study, "The Quantitative Estimation of Silica in Rice Husk Ash by Titrimetric Method : A Case Study for Uncertainty Calculation," **2010**.
16. Chindaprasirt, P.; Kanchanda, P.; Sathonsaowaphak, A.;. Cao, H. T., *Constr. Build. Mater.*, **2007**, *21*, 1356.
17. Chindaprasirt, P.; Jaturapitakkul, C.; Rattanasak, U., "Influence of fineness of rice husk ash and additives on the properties of lightweight aggregate," Fuel, **2009**, *88*, 158.
18. Ganesan, K.; Rajagopal, K.; Thangavel, K., *Constr. Build. Mater.*, **2008**, *22*, 1675.
19. Nehdi, M.; Duquette, J.; Damatty, A. El., *Cem. Concr. Res.*, **2003**, *33*, 1203.
20. Wang, G.; Wang, D.; Kuang, S.; Xing, W.; Zhuo, S., *Renew. Energy*, **2014**, *63*, 708.
21. Liou, T.; Wu, S., *Ind. Eng. Chem. Prod. Res. Dev.*, **2010**, *49*, 8379.
22. Zheng, J. L.; Kong, Y. P., *Energy Convers. Manag.*, **2010**, *51*, 182.
23. Cobreros C., et al., *BioResources*, **2015**, *10*, 3757.
24. Shih, J. Y.; Chang, T. P.; Hsiao, T. C., *Mater. Sci. Eng. A*, **2006**, *424*, 266.
25. Jo, B. W.; Kim, C. H.; Lim, J. H., *ACI Mater. J.*, **2007**, *104*, 404.
26. Liou, T.H., *Mater. Sci. Eng. A*, **2004**, *364*, 313.
27. Pijarn, N.; Jaroenworaluck, A.; Sunsaneeyametha, W.; Stevens, R., *Powder Technol.*, **2010**, *203*, 462.
28. Liou, T. H., "Evolution of chemistry and morphology during the carbonization and combustion of rice husk," Carbon N. Y., **2004**, *42*, 785.
29. Singh, D.; Kumar, R.; Kumar, A.; Rai, K. N., M. S. Programme, and M. Engineering, "Synthesis and characterization of rice husk silica, silica-carbon composite and H3PO4 activated silica," Cerâmica, **2008**, *54*, 203.
30. Yalçin, N.; Sevinç, V., *Ceram. Int.*, **2001**, *27*, 219.
31. Martínez, J. D.; Pineda, T.; López, J. P.; Betancur, M., "Assessment of the rice husk lean-combustion in a bubbling fl uidized bed for the production of amorphous silica-rich ash," *Energy*, **2011**, *36*, 3846.
32. Mochidzuki, K.; Sakoda, A.; Suzuki, M.; Izumi, J., *Ind. Eng. Chem.*, **2001**, *40*, 5705.
33. Salavati-Niasari, M.; Javidi, J.; Dadkhah, M., *Comb. Chem. High Throughput Screen.*, **2013**, *16*, 458.
34. Hincapié-Rojas, Fernando, Daniel; *Green Mater.*, **2018**, 1.
35. Mansaray, K. G.; Ghaly, A. E., *Bioresour. Technol.*, **1998**, *65*, 13.
36. Sun, K.; Jiang, J., *Biomass and Bioenergy*, **2010**, *34*, 539.
37. Ruksudjarit, A.; Rujijanagul, G.; *Adv. Mater. Res.*, **2008**, 649.
38. Affandi, S.; Setyawan, H.; Winardi, S.; Purwanto, A.; Balgis, R., *Adv. Powder Technol.*, **2009**, *20*, 468.
39. Kalapathy, J. S. U.; Proctor, A., *Technol. Bioresour.*, **2000**, *8524*, 257,
40. Bernal-Correa, R.; Rosales-Rivera, A.; Pineda-Gómez, P.; Salazar, N. A., *J. Alloys Compd.*, **2010**, *495*, 491.
41. Obinson, I. R., *J. Phys. Soc. Japan*, **2013**, *82*, 1.

